

Calcareous nannofossil changes during the late Callovian–early Oxfordian cooling phase

Fabrizio Tremolada^{a,*}, Elisabetta Erba^b, Bas van de Schootbrugge^c,
Emanuela Mattioli^d

^a Geological Sciences Department, Rutgers, The State University of New Jersey, 610 Taylor Road, Piscataway, NJ 08854, USA

^b Earth Sciences Department “Ardito Desio”, University of Milan, via Mangiagalli 34, 20133 Milano, Italy

^c Geological and Paleontological Institute, Johann Wolfgang Goethe University, Senckenberganlage 32-34, Frankfurt am Main D-60054, Germany

^d Université Claude Bernard Lyon 1, UMR 5125-CNRS, Laboratoire PEPS, UFR de Sciences de la Terre, 2 rue Dubois, 69622 VILLEURBANNE Cedex, France

Received 15 November 2005; received in revised form 20 February 2006; accepted 20 February 2006

Abstract

Calcareous nannofossil quantitative and biostratigraphic analyses integrated with carbon and oxygen stable isotopes were carried out on the core ANDRA (Agence Nationale pour la gestion des Déchets Radio-Actifs—FRANCE) HTM 102 across the Callovian/Oxfordian boundary drilled at Cirfontaines-en-Ornois, Département de Haute-Marne, eastern France. Calcareous nannofossil assemblages at the Callovian–Oxfordian transition are dominated by the genus *Watznaueria*. An increase in abundance of *Biscutum* spp. and A-group, which consists of *Axopodorhabdus* spp. (*A. atavus*, *A. rahla*, and *A. cylindratus*), *Podorhabdus grassei*, *Octopodorhabdus decussatus*, *Hexapodorhabdus cuvillieri* (family Axopodorhabdaceae), and *Triscutum* spp., correlates with a significant positive excursion in $\delta^{18}\text{O}$ suggesting that these groups were probably adapted to cooler surface waters. A positive increase in $\delta^{13}\text{C}$ values is coupled with high abundances of eutrophic taxa such as *Zeughrabdotus erectus*, *Biscutum* spp., and small-sized *Watznaueria britannica*, and a decrease in abundance of the big and oligotrophic taxa *Schizosphaerella punctulata* and *Watznaueria manivittae*. Climate cooling across the Callovian/Oxfordian boundary probably triggered a breakdown in stratification of surface waters leading to more intense nutrient recycling and higher primary productivity that favoured the shift in abundance of small-sized eutrophic taxa in the East Paris Basin.

© 2006 Elsevier B.V. All rights reserved.

Keywords: Callovian–Oxfordian transition; calcareous nannofossils; climatic changes; primary productivity

1. Introduction

The long-held paradigm that the Mesozoic was essentially ice-free and characterized by warm and equable climate conditions is slowly crumbling as more and more

evidence is presented for cold interludes of the Mesozoic Greenhouse. Relatively colder intervals have now been identified during the Aptian–Albian, the Valanginian and the Pliensbachian (Weissert and Lini, 1991; Price, 1999; Hochuli et al., 1999; Melinte and Mutterlose, 2001; Herrle and Mutterlose, 2003; Pucéat et al., 2003; McArthur et al., 2004; Erba et al., 2004; Weissert and Erba, 2004; Rosales et al., 2004; Van de Schootbrugge et al., 2005). A

* Corresponding author. Tel.: +1 732 445 0688; fax: +1 732 445 3374.
E-mail address: ftremola@rci.rutgers.edu (F. Tremolada).

pronounced climatic deterioration has also been identified across the Callovian/Oxfordian (C/O) boundary (~161.2 Ma; Gradstein et al., 2004). Both isotopic and paleontological data provide evidence for a climatic perturbation. The temperature fall begun in the Late Callovian (uppermost *Peltoceras athleta* ammonite zone) and lasted ~2.6 My through the Early Oxfordian (Dromart et al., 2003a). Oxygen–isotope ratios of belemnite rostra from Russia, Poland and Britain suggest a 6–7 °C temperature decrease (e.g., Podlaha et al., 1998; Barskov and Kiyashko, 2000; Jenkyns et al., 2002). A decrease in temperatures is also recorded in the oxygen isotope compositions of phosphate from vertebrate tooth enamel (Lécuyer et al., 2003). Philippe and Thevenard (1996) documented the presence of the presumably Boreal gymnosperm genus *Xenoxylon* in the Upper Callovian and Lower Oxfordian of Germany and France, while palynomorphs described from the North Sea Basin are indicative of cool and humid conditions (Abbink et al., 2001). Boreal ammonites such as the Cardioceratidae and Kosmoceratidae were observed in southeastern France (e.g., Fortwengler, 1989), Georgia (Topchishvili et al., 1998), Iran (Seyed-Emani et al., 1995) and Montana (Poulton et al., 1992). In addition, sedimentological investigations in northeastern Asia reveal the presence of glendonite (Chumakov and Frakes, 1997), a pseudo-

morph of calcite that forms exclusively in subaqueous conditions not higher than ~0 °C. The presence of glendonites may suggest the formation of continental ice caps at the North pole during this time interval (e.g., Dromart et al., 2003a,b). However, it is still unclear if this cooling event only had a regional to supraregional (e.g., the Eurasia supercontinent) or a global extent owing to our limited knowledge about Callovian–Oxfordian paleoclimate changes in the Southern Hemisphere. This long-term climatic deterioration might have been caused by intensified organic carbon burial in the Middle Callovian triggering a drawdown in atmospheric CO₂ concentrations (Dromart et al., 2003a).

Here, we document major changes in calcareous nannofossil assemblages recorded in the East Paris Basin during this critical interval of late Middle Jurassic to early Late Jurassic. The Paris Basin was characterized by shallow-water depositional environments (~200 m) and three main carbonate platform domains: Burgundy, Normandy, and Ardennes during Middle and Late Jurassic. The Paris Basin represents the northwestern part of the Tethys Ocean (Lécuyer et al., 2003). Nannofloral communities and fossil phytoplankton communities in general are affected by changes in trophic and thermal regime and their fluctuations in abundance can be interpreted to reflect climatic and paleoceanographic

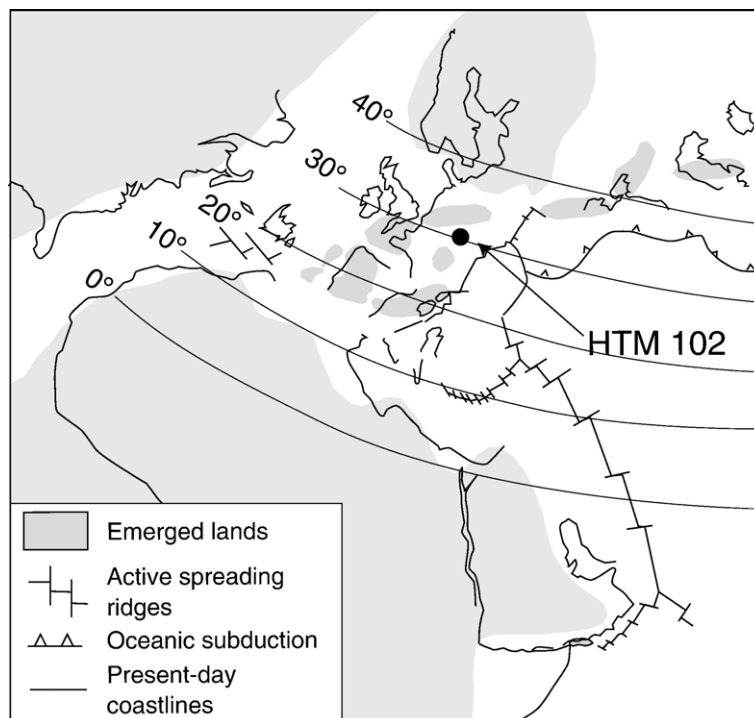


Fig. 1. Paleogeographic map at 161 Ma (from Cecca et al., 2005, modified) and location of borehole ANDRA HTM 102.

variations of surface waters. This study also represents the first attempt to link the calcareous nannofossil response to the climatic refrigeration at the Callovian–Oxfordian (C–O) transition. To achieve these aims, we combine quantitative nannofossil data with bulk carbonate $\delta^{13}\text{C}$ and $\delta^{18}\text{O}$ measurements. $\delta^{18}\text{O}$ fluctuations were analyzed in order to detect the onset and the progression of cooling conditions that characterize the C–O transition. The $\delta^{13}\text{C}$ record is used to monitor changes in the carbon cycle in this interval.

2. Materials and methods

Isotopic and micropaleontological (biostratigraphic and quantitative) analyses were carried out on 56 and 70 samples, respectively, collected from the ANDRA (Agence Nationale pour la gestion des Déchets Radio-Actifs) borehole HTM 102 drilled at Cirfontaines-en-Ornois (~70 km from Nancy; 48°26'53"N, 05°22'58" E), in eastern France (Fig. 1). This area was a peritidal environment with a paleolatitude of ~30°N. Drilling operations (recovery=100%) were performed by Sedco-Forax, whereas lithological and lithostratigraphic analyses were carried out by ANTEA/BRGM. All information regarding the borehole must be requested to the geological division of ANDRA (<http://www.andra.fr>). Cores are stored in the ANDRA plant at Bure, near Joinville, eastern France. We investigated the interval from 450.84 to 366.12 m below well head (mbwh). Green marlstones characterize the studied sedimentary succession between 450.84 and 436.75 mbwh, whereas the upper interval consists of dark claystones. These sediments correspond to the “Argiles de la Woëvre” Formation (Pellenard et al., 2003).

Calcareous nannofossils were analyzed in smear slides prepared from all lithologies under a light microscope at 1250× magnification. In order to obtain relative abundances, at least 300 specimens were counted in each slide. All specimens were identified at the species level and, then, grouped at the generic level with the exception of *Zeughrabdotus erectus* and *Schizosphaerella punctulata*. Groupings include *Watznaueria* spp. (*W. barnesiae*, *W. fossacincta*, *W. britannica*, and *W. manivittae*), *Cyclagelosphaera* spp. (mostly *C. margerelii* with minor abundances of *C. tubulata* and *C. deflandrei*), and *Biscutum* spp. (mainly *B. constans* with minor percentages of *B. dorsetensis* and *B. dubium*). Taxa such as *Axopodorhabdus* spp. (*A. atavus*, *A. rahla*, and *A. cylindricus*), *Podorhabdus grassei*, *Octopodorhabdus decussatus*, and *Hexapodorhabdus cuvillieri* (family Axopodorhabdaceae), and *Triscutum* spp. display the same distribution patterns and are grouped together in the A-group. In

addition, all specimens observed in 20 microscope fields of view (FOV) of *Biscutum* spp. and A-group were counted. This method was used to estimate if fluctuations in abundance of *Biscutum* spp. and A-group are independent from variations in abundance of other groupings. The nannofossil preservation was evaluated by using the categorization of Bown and Young (1998). Principal Component Analysis (PCA, Varimax-orthogonal transformation method) and scattered plots were carried out by using the statistical software Stat-View 5.0. The method to extract factors was eigenvalues.

Carbon and oxygen isotope analyses were carried out on the bulk carbonate fraction using a VG Optima mass spectrometer with a Multiprep peripheral attached for the automated analysis of CaCO_3 samples at Rutgers University. Samples were dried overnight and crushed. Approximately 500 μg of sediment was loaded into reaction vials for analysis. Values are reported versus Vienna-PDB using NBS-19 and an internal lab standard. The 1-sigma standard deviations of $\delta^{18}\text{O}$ and $\delta^{13}\text{C}$ values from the standards analyzed during the sample runs are 0.08‰ and 0.04‰, respectively.

3. Results

3.1. Calcareous nannofossils

Calcareous nannofossil specimens are abundant and display a moderate to good preservation throughout the investigated interval. In general, calcareous nannofossil assemblages are slightly etched (E1) and/or overgrown (O1; see “supplementary material”). A few samples are characterized by moderate etching (E2) and overgrowth (O2). Our biostratigraphic analysis on the same samples used for quantitative investigations shows that the studied interval spans from nannofossil Zones NJ13 through NJ15a (Fig. 2) adopting the biozonation of Bown and Cooper (1998). The identified nannofossil Zones encompass the C/O boundary and represent ~3 My. The bottom of the studied section is assigned to the NJ13 nannofossil Zone owing to the presence of the zonal marker *Stephanolition bigotii* and the absence of *Stephanolition bigotii maximum*. The First Occurrence (FO) of *S. bigotii maximum* lies at 436.6 mbwh, whereas its Last Occurrence (LO) is recorded at 409.69 mbwh. These events define the base of NJ14 and NJ15a nannofossil Zones, respectively. The top of the section is assigned to the NJ15a nannofossil Zone based on the presence of *Lotharingius crucicentralis*, whose LO marks the base of NJ15b nannofossil Zone.

Our quantitative analyses reveal fairly remarkable changes in calcareous nannofossil assemblages across

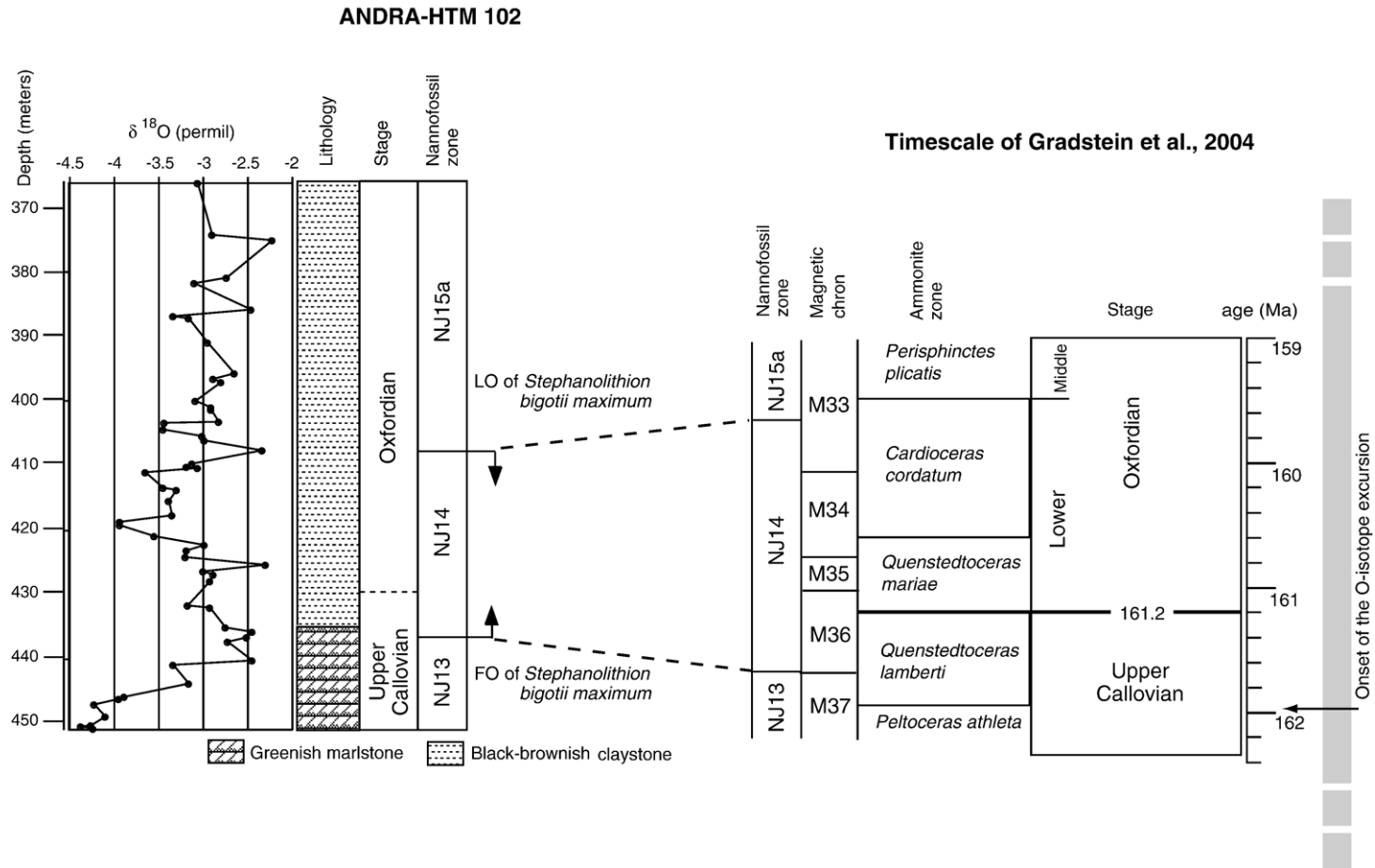


Fig. 2. Calcareous nannofossil events and nannofossil zones (after Bown and Cooper, 1998) recorded in borehole ANDRA HTM 102, and correlation with the timescale of Gradstein et al. (2004). The Callovian/Oxfordian boundary has been tentatively placed using the $\delta^{18}\text{O}$ anomaly as dated by Dromart et al. (2003b), Lécuyer et al. (2003), and Podlaha et al. (1998). The gray bar indicates the interval (Bathonian to Kimmeridgian) investigated by Dromart et al. (2003b), Lécuyer et al. (2003), and Podlaha et al. (1998).

the C–O transition (see “supplementary material”). Species richness ranges from 19 to 24 with small fluctuations. The nannofossil assemblage is overwhelmingly dominated by the genus *Watznaueria*, which comprises 63% to 81% of the total nannofossil assemblage (Fig. 3). The percentages of *W. barnesiae* and *W. fossacincta* range from 35% to 55% of the total assemblage. The taxon *W. manivitae* shows a fairly marked decrease in abundance from the bottom (~19% of the total assemblage) to the top of the section (5% on average of the total assemblage). Conversely, *W. britannica* increases progressively towards the top of the section (from 13 to 25% of the total assemblage) with no striking fluctuations. Interestingly, the taxon *W. britannica* is mostly represented by small specimens (5–5.5 μm) above 443.88 mbwh. The taxon *S. punctulata* has a continuous occurrence in the lower part of the section, although its percentages are fairly low (<5%). From 443.88 mbwh to the top of the section this taxon is rare or absent. Abundances of the *Cyclagelosphaera* group are low and do not exceed 3% on average (Fig. 3). The percentages of the dissolution-susceptible taxon *Z. erectus* display small oscillations and range from 2% to 7% (Fig. 4). The most marked fluctuations in abundance concern the taxon *Biscutum* and the A-group. Both groups are absent in the lower part of the section, but increase in abundance from 443.88 mbwh (Fig. 4). The genus *Biscutum* ranges from 5% to 18% in the middle and upper part of the section with the highest percentages between 427 and 422 mbwh (mean = 14%). The distribution pattern of the A-group broadly matches that of *Biscutum*, although its percentages are much lower (<8% of the total assemblage). The correlation between these groupings is emphasized by the high value of R^2 (Fig. 5a). Abundances per 20FOV of *Biscutum* spp. and A-group show a similar trend. Both *Biscutum* and A-group are absent in the lower part of the section, but increase abruptly above 443.88 mbwh. The abundances per FOV of *Biscutum* and A-group in the middle and upper part of the core range from 59 to 127 specimens/20FOV and from 14 to 73 specimens/20FOV, respectively (Fig. 6).

Other taxa such as *Stephanolithion* spp., *Tubirhabdus patulus*, *Lotharingius* spp., *Crepidolithus* spp., *Ansulosphera* spp., and *Discorhabdus* spp. combined account for <8% of the total nannofossil assemblages. These taxa are grouped in the “other species” group (see “supplementary material”).

The PCA method was applied to percentage values of individual taxa recorded in borehole HTM 102. Factor 1, loading on *S. punctulata* and *W. manivitae* in opposition with *W. britannica* and, partly, *Biscutum* and A-group,

probably corresponds to nutrient concentrations (Fig. 7). Factor 2, in which *W. barnesiae* is opposed to *Biscutum* and A-group, may correspond to temperature (Fig. 7).

3.2. Geochemistry

Bulk rock carbonate carbon isotope ($\delta^{13}\text{C}_{\text{carb}}$) values generally ranges from 1.11‰ to 2.29‰, although a few samples recorded at 447.1 mbwh (0.89‰), at 435.84 mbwh (0.41‰), and at 407.54 mbwh (2.59‰) display anomalous $\delta^{13}\text{C}_{\text{carb}}$ values (Fig. 3). The $\delta^{13}\text{C}_{\text{carb}}$ signature shows a positive increase of 1.5‰, reaching +2.5‰ at the top of nannofossil Zone NJ14. After that, values taper off and remain steady around +2‰ towards the top of nannofossil Zone NJ15.

The bulk carbonate oxygen isotope signal records the most marked changes. The lower part of nannozone NJ13 is characterized by the lowest values (mean = -4.20‰). A major positive $\delta^{18}\text{O}_{\text{carb}}$ shift (mean = -2.95‰) is observed from 443.88 mbwh to the top of the section. This interval is characterized by pronounced $\delta^{18}\text{O}_{\text{carb}}$ fluctuations ranging from -2.23‰ to -3.94‰. In particular, the negative $\delta^{18}\text{O}_{\text{carb}}$ shift at 419.2 mbwh ($\delta^{18}\text{O}_{\text{carb}}$ value = -3.94‰) correlates with a decrease in relative abundance of *Biscutum* spp. and A-group.

4. Discussion

4.1. Preservation and diagenesis

Fluctuations in abundance and composition of calcareous nannofossil assemblages can be interpreted as the response of phytoplankton to paleoceanographic and paleoclimatic changes. Calcareous nannofossil communities at the Callovian–Oxfordian transition in the ANDRA HTM 102 drillcore are dominated by the genus *Watznaueria*. Early Cretaceous (calcareous) phytoplankton assemblages showing percentages of the taxon *Watznaueria* (especially *W. barnesiae*) higher than 40% (e.g., Thierstein, 1981; Thierstein and Roth, 1991; Roth and Bowdler, 1981; Williams and Bralower, 1995) indicate intense diagenetic alteration and dissolution of fragile taxa. However, the Bathonian–Kimmeridgian interval is characterized by the dominance of the genus *Watznaueria* (Busson et al., 1992; Bown and Cooper, 1998; Pittet and Mattioli, 2002; Olivier et al., 2004). In addition, Lees et al. (2004) documented blooms of *Watznaueria* in pristinely preserved nannofossil assemblages from the Upper Jurassic Kimmeridge Clay Formation. This dominance possibly reflects a real ecological signal rather than diagenetic overprint. The small degree of etching and overgrowth, and negligible

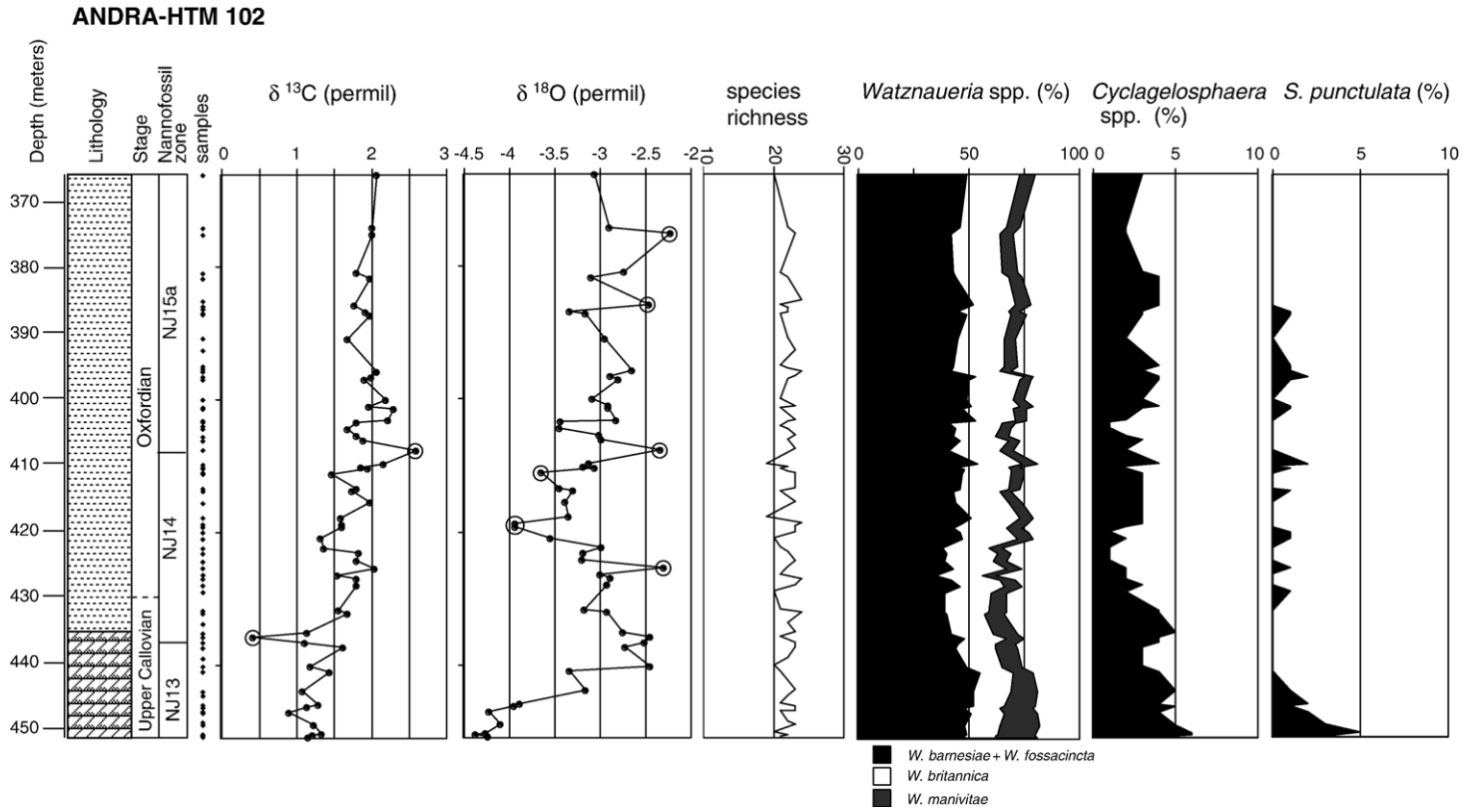


Fig. 3. C- and O-isotope fluctuations (‰), species richness, and percentages of *Watznaueria* spp., *S. punctulata*, and *Cyclagelosphaera* spp. Circled data-points represent $\delta^{13}\text{C}_{\text{carb}}$ and $\delta^{18}\text{O}_{\text{carb}}$ values that may result from diagenetic alteration.

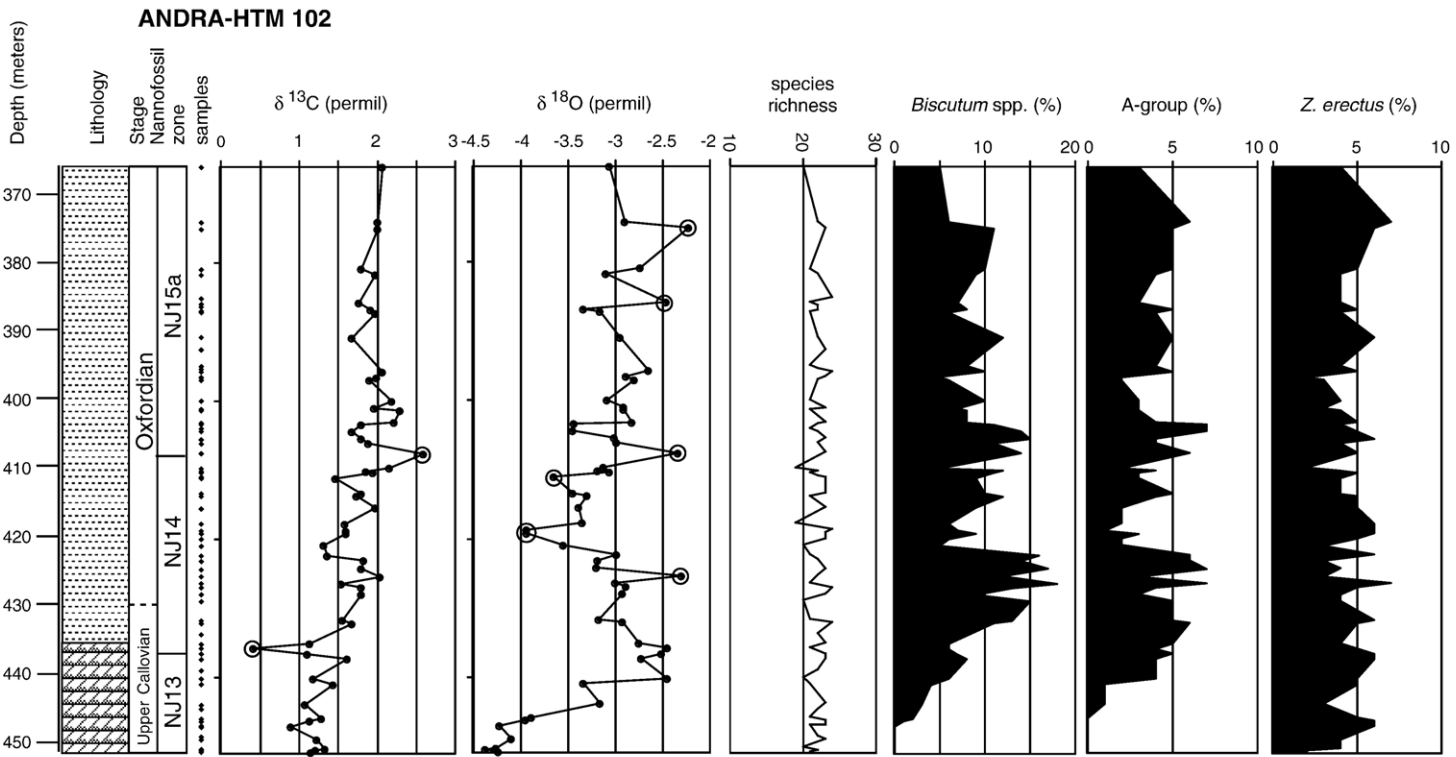


Fig. 4. C- and O-isotope fluctuations (‰), species richness and percentages of *Z. erectus*, *Biscutum* spp., and A-group. Circled data-points represent $\delta^{13}\text{C}_{\text{carb}}$ and $\delta^{18}\text{O}_{\text{carb}}$ values that may result from diagenetic alteration.

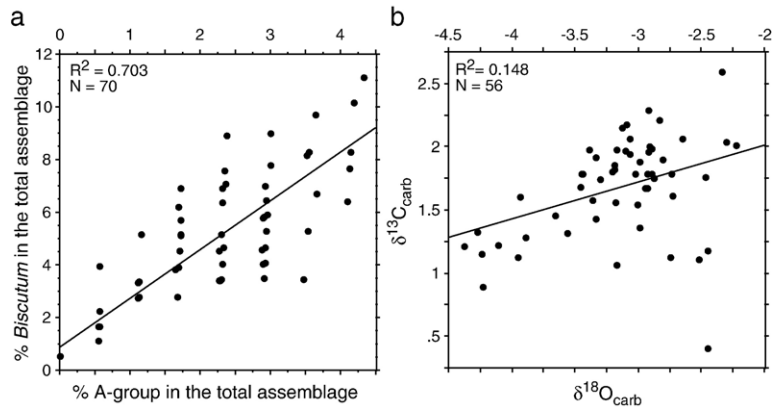


Fig. 5. a) Scattered plot showing a good correlation between percentages of *Biscutum* spp. and A-group; b) $\delta^{13}\text{C}_{\text{carb}}$ vs. $\delta^{18}\text{O}_{\text{carb}}$.

fluctuations in species richness may suggest a slight diagenetic alteration throughout the section. In addition, significant abundances of dissolution-susceptible species such as *Z. erectus* and *Biscutum* spp. indicate that nanofossil fluctuations are only moderately affected by diagenesis. The absence of the dissolution-susceptible taxa *Biscutum* spp. and A-group in the lower part of the section may result from diagenetic alteration. However, the extremely fragile taxon *Z. erectus* shows moderate, but noteworthy, abundances in the same interval. The loose and open construction of *S. punctulata* nannolith makes this taxon susceptible to preferential destruction by dissolution because the majority of the surface area of each crystallite is exposed to pore fluids. The highest abundances of *S. punctulata* were observed between 450.84 and 443.88 mbwh suggesting minor diagenetic alteration. Consequently, the absence of *Biscutum* spp. and A-group between 450.84 and 443.88 mbwh cannot be ascribed to diagenetic removal, and the shift in abundance recorded from 443.88 mbwh presumably represents a primary paleoenvironmental signal.

The $\delta^{13}\text{C}_{\text{carb}}$ and $\delta^{18}\text{O}_{\text{carb}}$ records represent a function of changes in regional and/or global paleoceanographic changes (primary productivity, seawater pH, temperature, salinity and shifts in the fractions of organic and inorganic carbon burial), changes in carbonate mineralogy (i.e., calcite and aragonite), assemblage composition (i.e., changes in nanofossil abundance), and diagenetic overprint. The burial history mainly regulates the extent of diagenetic alteration on both $\delta^{18}\text{O}_{\text{carb}}$ and $\delta^{13}\text{C}_{\text{carb}}$. In particular, calcite cement precipitated during deep burial diagenesis alters the O-isotope compositions of bulk carbonates resulting in lighter $\delta^{18}\text{O}$ values (e.g., Marshall, 1992; Schrag et al., 1995). Bulk carbon- and oxygen-isotopes are also influenced by different degrees of isotopic fractionation exerted by vital effects of

individual calcareous nanofossil species (Dudley and Goodney, 1979; Dudley et al., 1986; Ziveri et al., 2003). Carbon- and oxygen-isotope records in hole HTM 102 match the $\delta^{18}\text{O}_{\text{carb}}$ and $\delta^{13}\text{C}_{\text{carb}}$ fluctuations observed in different localities, characterized by different burial histories, of the Eurasia supercontinent derived from belemnites, shark teeth, molluscs and bulk rock carbonates (e.g., Podlaha et al., 1998; Barskov and Kiyashko, 2000; Jenkyns et al., 2002; Padden et al., 2002; Malchus and Steuber, 2002; Lécuyer et al., 2003; Wierzbowski, 2004). The correlation between $\delta^{18}\text{O}_{\text{carb}}$ and $\delta^{13}\text{C}_{\text{carb}}$ is low ($R^2 = 0.148$; Fig. 5b) suggesting a minor influence of diagenesis. Nanofossil assemblages are dominated by *Watznaueria* throughout the studied section suggesting a minor influence of the vital effect of individual species. As a result, we think that the overall trend of both $\delta^{18}\text{O}_{\text{carb}}$ and $\delta^{13}\text{C}_{\text{carb}}$ reflects a true primary signal, although a few anomalous values in both $\delta^{18}\text{O}_{\text{carb}}$ and $\delta^{13}\text{C}_{\text{carb}}$ may suggest some diagenetic alteration.

4.2. Paleoceanography

The oxygen isotope fluctuations clearly indicate major variations in temperature during the Callovian–Oxfordian transition in the East Paris Basin that are in agreement with previously reported changes in paleoclimate across this interval. However, because the oxygen isotopic composition of early Late Jurassic seawater (δ_{v}) is unknown, we can neither calculate absolute paleotemperatures nor exclude concurrent changes in salinity. Low $\delta^{18}\text{O}$ values recorded in the lower part of the section are indicative of warmer conditions and/or lower salinity. An abrupt shift towards lower temperatures and/or higher salinities characterizes the interval from 443.88 mbwh to the top of the section and may be the combined effect of cooling and the storage of the

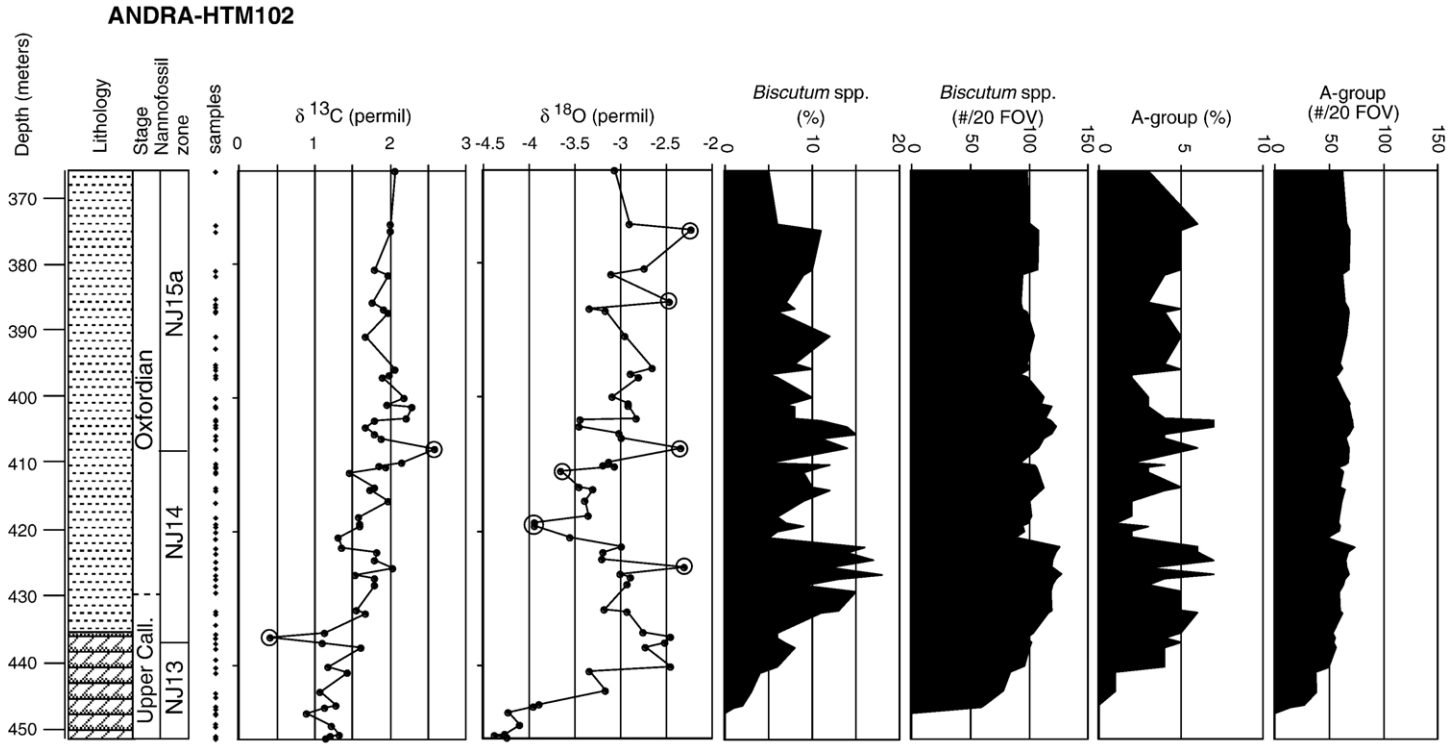


Fig. 6. Abundances (#specimens/20FOV and percentages of the total nannofossil assemblage) of *Biscutum* spp. and A-group plotted against C- and O-isotope fluctuations (%). Circled data-points represent $\delta^{13}\text{C}_{\text{carb}}$ and $\delta^{18}\text{O}_{\text{carb}}$ values that may result from diagenetic alteration.

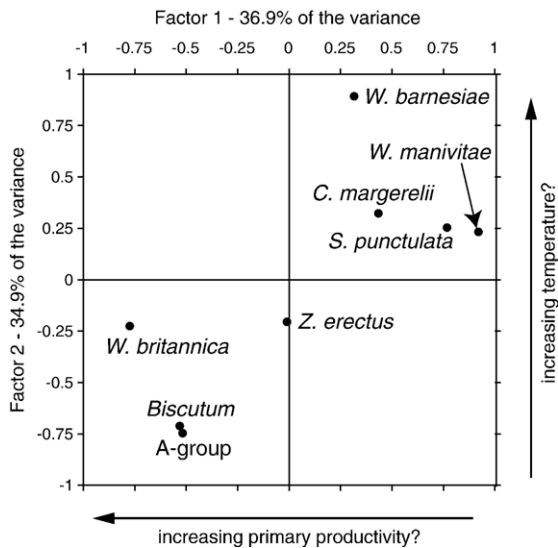


Fig. 7. Principal Component Analysis (PCA) applied to percentages of calcareous nannofossil indicate possible ecological affinities of different taxa. An orthogonal factor was selected. Factors are eigenvalues.

lighter ^{16}O isotope in continental ice-caps. According to Lécuyer et al. (2003), changes in salinity can only partially explain the shift in $\delta^{18}\text{O}$ values because no evidence for excessive evaporation over precipitation is provided by the sedimentary record in the Paris Basin. In addition, our O-isotope data correlate with temperature reconstructions inferred from palynological proxies in Northern Europe (Abbinck et al., 2001).

The slight increase in $\delta^{13}\text{C}$ values recorded across the C–O transition might have been indirectly caused by the cooling. The $\delta^{13}\text{C}$ fluctuations are controlled by the partitioning of the global carbon pool between reduced (organic carbon) and oxidized (carbonate, carbon dioxide and bicarbonate) reservoirs. The temperature fall presumably reduced the stratification of water masses favouring a more intense nutrient recycling in the East Paris Basin area. Higher nutrient concentrations stimulated the primary productivity in photoautotrophic organisms.

4.3. Paleoecology

Fluctuations in abundance and composition of calcareous nannofossil assemblages could be interpreted as the response of phytoplankton to paleoceanographic and paleoclimatic changes highlighted by stable isotope investigations. The positive $\delta^{18}\text{O}$ excursion correlates with the shift in abundance of *Biscutum* (especially *B. constans*) and A-group, while these groups are absent or rare in the lower part of the section characterized by the lowest $\delta^{18}\text{O}$ values (Fig. 4). This relationship may

suggest that these taxa flourish with low temperatures. Our results may thus support the observations of Herrle (2003) in Middle Cretaceous sections regarding the affinity of *B. constans* for cold waters. *S. punctulata* displays an inverse correlation with the abundances of *Biscutum* and the A-group. The temperature affinities of *S. punctulata* remain unclear, however, this species is generally more abundant at lower latitudes (Bucefalo Palliani et al., 2002). Moreover, in the latest Oxfordian–earliest Kimmeridgian of SW Germany, a progressive increase in relative abundance of *S. punctulata* is recorded, and correlates to a shift from humid conditions in the earliest Late Oxfordian to a drier and warmer climate in the earliest Kimmeridgian (Bartolini et al., 2003). *S. punctulata* is rare or absent during the cooling phase in core ANDRA HTM 102 (Fig. 3). Other taxa do not correlate significantly with $\delta^{18}\text{O}$ fluctuations and seem to be unrelated to climatic variations.

The taxa *Z. erectus* and *B. constans* are interpreted as indices of higher fertility of surface waters because of their high abundances in C_{org} -rich sediments and paleo-upwelling areas (e.g., Roth and Bowdler, 1981; Roth and Krumbach, 1986; Premoli Silva et al., 1989; Watkins, 1989; Erba, 1992; Erba et al., 1992) and results derived from statistical analyses (Herrle, 2003; Tremolada et al., in press). Significant variations in the abundances of *Z. erectus* and *Biscutum* (especially *B. constans*) spp. and the decrease in percentages of *S. punctulata* may indicate higher primary productivity. The taxon *S. punctulata* is thought to flourish when the nutricline was deep and surface-waters were characterized by enhanced oligotrophy (Claps et al., 1995; Cobianchi and Picotti, 2001; Mattioli and Pittet, 2002; Pittet and Mattioli, 2002; Bartolini et al., 2003; Olivier et al., 2004; Erba, 2004). Other authors have interpreted *S. punctulata* as an opportunistic taxon that thrived under intense vertical mixing (Mattioli, 1997; Walsworth-Bell, 2001) or profited from sporadic pulses of nutrients in oligotrophic environments (Mattioli and Pittet, 2004). However, the inverse correlation between eutrophic species and *S. punctulata* implies that the latter taxon may possibly be adapted to oligotrophic conditions of surface waters (Tremolada et al., 2005). Furthermore, increasing primary productivity could be indicated by the slight decrease in abundance of *W. manivitae* and the increase in percentage of small-sized *W. britannica* towards the top of the section. The taxon *W. manivitae* displays the same trend of *S. punctulata* in the Late Jurassic of SW Germany, possibly indicating similar ecological preferences (low nutrient concentrations, warmer climate; Bartolini et al., 2003). *W. manivitae*

has been interpreted as the most oligotrophic component of the trophic preference continuum formed by the Watznaueriaceae plexus (Pittet and Mattioli, 2002). The dissolution-resistant genus *W. barnesiae* is a cosmopolitan taxon and its high quantities in moderately to well-preserved nannofossil assemblages are generally interpreted as indicative of oligotrophic surface waters (e.g., Roth and Krumbach, 1986; Premoli Silva et al., 1989; Williams and Bralower, 1995; Burns and Bralower, 1998). In addition, the abundances of *W. barnesiae* are generally in “phase opposition” with those of eutrophic taxa such as *Z. erectus* and *B. constans* (Erba et al., 1992; Herrle, 2003; Tremolada et al., in press). Conversely, Lees et al. (2004) interpreted blooms of *W. barnesiae* in the Kimmeridge Clay Formation as indicative of enhanced primary productivity. This taxon might be representative of more eutrophic conditions than *W. britannica* or *C. margerelii* (Lees et al., 2004). Olivier et al. (2004) in the Late Oxfordian/Early Kimmeridgian of SW Germany recognized three different-sized morphotypes of *W. britannica*. The largest morphotypes display similar ecological preferences as *W. manivitae* and *S. punctulata* (oligotrophic conditions), conversely, the smallest morphotypes covary with *B. dorsetensis* and *Z. erectus* (eutrophic conditions; Olivier et al., 2004). *C. margerelii* occupied an intermediate position in the trophic preference continuum described by Pittet and Mattioli (2002). Busson et al. (1992, 1993) have described high-abundance, low-diversity assemblages composed essentially of *C. margerelii* and *W. britannica* (= *Ellipsagelosphaera communis* in Busson et al., 1992) in a Late Jurassic restricted-lagoon environment, possibly receiving fresh-water influxes. Monospecific assemblages formed by *C. margerelii* also characterize the light-coloured laminae in Kimmeridgian bituminous sediments of the French Jura, interpreted as being deposited in a lagoonal environment with significant salinity variations (Tribovillard et al., 1992). As *C. margerelii* survived the K/T boundary extinction event, it has been argued (Street and Bown, 2000; Bown et al., 2004) that it was likely a neritic taxon. In the studied drillcore, *C. margerelii* is never dominant in the nannofossil assemblage. However, the small, but probably significant decrease in relative abundance of this taxon, that matches the increase in $\delta^{18}\text{O}$ values recorded from 443.88 mbwh, might be possibly interpreted in terms of a slight increase in salinity. The shift in percentages of the A-group towards the top of the section and the positive correlation with *Biscutum* might suggest meso-eutrophic affinities for this group. Further analyses in

different latitudinal settings are required to clarify the paleoecological affinities of the A-group and separate the influence of temperature and nutrients on calcareous nannofossil distribution patterns.

5. Conclusions

Stable isotopes and calcareous nannofossil abundances represent a primary signal only slightly altered by diagenetic overprint. Quantitative analyses performed on calcareous nannofossils show fairly marked changes in abundance and composition of nannofossil communities, although the genus *Watznaueria* account for ~ 70% of the total assemblage. The increase in abundance (relative and per 20FOV) of *Biscutum* spp. (mostly *B. dorsetensis* and *B. constans*) and A-group correlates with a $\delta^{18}\text{O}$ shift towards higher values. This result coupled with the decrease of warm water-adapted taxa such as *S. punctulata* and *W. manivitae* may suggest that *Biscutum* spp. and A-group are more adapted to cooler surface waters. C-isotope data show a small and continuous increase in $\delta^{13}\text{C}$ values. Cooling conditions probably led to the reduced stratification of water masses that favoured a slight increase in primary productivity via intensified nutrient recycling and upwelling. This scenario fits well with the decrease in percentages of oligotrophic taxa such as *S. punctulata* and *W. manivitae*, and the shift in abundance of *Biscutum* spp. and small-sized specimens of *W. britannica*, which are also regarded as indicative of eutrophic conditions.

Acknowledgements

Samples investigated in this study were provided by ANDRA (Agence Nationale pour la gestion des Déchets Radio-Actifs—FRANCE). C. Aurière (ANDRA), H. Rêbours (ANDRA), and M.P. Aubry (Rutgers University) are warmly thanked for their help in sampling operations and logistics. Stable isotopes were measured with the assistance of J.D. Wright (Rutgers University). This paper benefited from reviews by E. Thomas, P. Bown, and an anonymous reviewer. FT is supported by NSF (OCE-0084032) and Von Humboldt Foundation, EE by Cofin 2003 (no. 2003041915_001), and EM by ECLIPSE II.

Appendix A. Supplementary material

Supplementary data associated with this article can be found, in the online version, at doi:10.1016/j.marmicro.2006.02.007.

References

- Abbink, O., Targarona, J., Brinkhuis, H., Visscher, H., 2001. Late Jurassic to earliest Cretaceous palaeoclimatic evolution of the southern North Sea. *Glob. Planet. Change* 30, 231–256.
- Barskov, I.S., Kiyashko, S.I., 2000. Thermal regime variations in the Jurassic marine basin of the East European Platform at the Callovian/Oxfordian boundary: evidence from stable isotopes in belemnite rostra. *Doklady Earth Sci.* 372, 643–645.
- Bartolini, A., Pittet, B., Mattioli, E., Hunzicker, J., 2003. Regional control on stable isotope signature in deep-shelf sediments: an example of the Late Jurassic of southern Germany (Oxfordian–Kimmeridgian). *Sediment. Geol.* 160, 107–130.
- Bown, P.R., Cooper, M.K.E., 1998. Jurassic. In: Bown, P.R. (Ed.), *Calcareous Nannofossil Biostratigraphy*. Kluwer Academic Publishers, London, UK, pp. 34–85.
- Bown, P.R., Young, J.R., 1998. Techniques. In: Bown, P.R. (Ed.), *Calcareous Nannofossil Biostratigraphy*. Kluwer Academic Publishers, London, UK, pp. 16–28.
- Bown, P.R., Lees, J.A., Young, J.R., 2004. Calcareous nannoplankton evolution and diversity. In: Young, J.R., Thierstein, H.R. (Eds.), *Coccolithophores—From Molecular Processes to Global Impact*. Springer-Verlag, Berlin, Germany, pp. 481–508.
- Bucefalo Palliani, R., Mattioli, E., Riding, J.B., 2002. The response of marine phytoplankton and sedimentary organic matter to the Early Toarcian (Lower Jurassic) oceanic anoxic event in northern England. *Mar. Micropaleontol.* 46, 223–245.
- Burns, C.E., Bralower, T.J., 1998. Upper Cretaceous nannofossil assemblages across the Western Interior Seaway: implications for the origins of lithologic cycles in the Greenhorn and Niobrara Formations. *SEPM Spec. Publ., Concepts Sedimentol. Paleontol.* 6, 35–58.
- Busson, G., Noël, D., Cornée, A., 1992. Les coccolithes en “boutons de manchette” et la genèse des calcaires lithographiques du jurassique supérieur. *Rev. Paléobiol.* 11, 255–271.
- Busson, G., Noël, D., Contini, D., Mangin, A.M., Cornée, A., Hantzperg, P., 1993. Omniprésence de coccolithes dans des calcaires lagunaires du jurassique moyen et supérieur de France. *Bull. Cent. Rech. Explor. Prod. Elf-Aquitaine* 17, 291–301.
- Cecca, F., Martin Garin, B., Marchand, D., Lathuilière, B., Bartolini, A., 2005. Paleoclimatic control of biogeographic and sedimentary events in Tethyan and peri-Tethyan areas during the Oxfordian (Late Jurassic). *Palaeogeogr. Palaeoclimatol. Palaeoecol.* 222, 10–32.
- Chumakov, N.M., Frakes, L.A., 1997. Mode of origin of dispersed clasts in Jurassic shales: southern part of the Yana-Kolyma fold belt, NE-Asia. *Palaeogeogr. Palaeoclimatol. Palaeoecol.* 128, 77–85.
- Claps, M., Erba, E., Masetti, D., Melchiorri, F., 1995. Milankovitch-type cycles recorded in Toarcian black shales from the Belluno Trough (Southern Alps, Italy). *Mem. Sci. Geol.* 47, 179–188.
- Cobianchi, M., Picotti, V., 2001. Sedimentary and biological response to sea-level and palaeoceanographic changes of a Lower–Middle Jurassic Tethyan platform margin (southern Alps, Italy). *Palaeogeogr. Palaeoclimatol. Palaeoecol.* 169, 219–244.
- Dromart, G., Garcia, J.P., Picard, S., Atrops, F., Lécuyer, C., Sheppard, S.M.F., 2003a. Ice Age at the Middle–Late Jurassic Transition? *Earth Planet. Sci. Lett.* 213, 205–220.
- Dromart, G., Garcia, J.-P., Gaumet, F., Picard, S., Rousseau, M., Atrops, F., Lécuyer, C., Sheppard, S.M.F., 2003b. Perturbation of the Carbon cycle at the Middle/Late Jurassic transition: geological and geochemical evidence. *Am. J. Sci.* 303, 667–707.
- Dudley, W.C., Goodney, D.E., 1979. Oxygen isotope analyses of coccoliths grown in culture. *Deep-Sea Res., A* 26, 495–503.
- Dudley, W.C., Blackwelder, P., Brand, L., Duplessy, J.C., 1986. Stable isotopic composition of coccoliths. *Mar. Micropaleontol.* 10, 1–8.
- Erba, E., 1992. Middle Cretaceous calcareous nannofossils from the Western Pacific (ODP Leg 129): evidence for paleoequatorial crossings. *Sci. Res. ODP* 129, 189–201.
- Erba, E., 2004. Nannofossils and Mesozoic oceanic anoxic events. *Mar. Micropaleontol.* 52, 85–106.
- Erba, E., Castradori, D., Guasti, G., Ripepe, M., 1992. Calcareous nannofossils and Milankovitch cycles: the example of the Albian Gault Clay Formation (Southern England). *Palaeogeogr. Palaeoclimatol. Palaeoecol.* 93, 47–69.
- Erba, E., Bartolini, A., Larson, R.L., 2004. Valanginian “Weissert Oceanic Anoxic Event”. *Geology* 32, 149–152.
- Fortwengler, D., 1989. Les “Terres Noires” d’âge Callovien supérieur à Oxfordien moyen des chaînes subalpines du Sud: Paris. *C. R. Acad. Sci.* 308, 531–536.
- Gradstein, F.M., Ogg, J.G., Smith, A.G., Bleeker, W., Lourens, L., 2004. A new geological Time Scale with special reference to Precambrian and Neogene. *Episodes* 27, 83–100.
- Herrle, J.O., 2003. Reconstructing nutricline dynamics of mid-Cretaceous oceans: evidence from calcareous nannofossils from the Niveau Paquier black shale (SE France). *Mar. Micropaleontol.* 47, 307–321.
- Herrle, J.O., Mutterlose, J., 2003. Calcareous nannofossils from the Aptian–early Albian of SE France: Paleocceanographic and biostratigraphic implications. *Cretac. Res.* 24, 1–22.
- Hochuli, P.A., Menegatti, A.P., Weissert, H., Riva, A., Erba, E., Premoli Silva, I., 1999. Episodes of high productivity and cooling in the early Aptian Alpine Tethys. *Geology* 27, 657–660.
- Jenkyns, H.C., Jones, C.E., Gröcke, D.R., Hesselbo, S.P., Parkinson, D.N., 2002. Chemostratigraphy of the Jurassic System: applications, limitations and implications for paleoceanography. *J. Geol. Soc. (Lond.)* 159, 351–378.
- Lécuyer, C., Picard, S., Garcia, J.-P., Sheppard, S.M.F., Grandjean, P., Dromart, G., 2003. Thermal evolution of Tethyan surface during the Middle–Late Jurassic: evidence from 18 O values of marine fish teeth. *Paleoceanography* 18. doi:10.1029/2002PA000863.
- Lees, J.A., Bown, P.R., Young, J.R., Riding, J.B., 2004. Evidence for annual records of phytoplankton productivity in the Kimmeridge Clay Formation coccolith stone bands (Upper Jurassic, Dorset, UK). *Mar. Micropaleontol.* 52, 29–49.
- Malchus, N., Steuber, T., 2002. Stable isotope records (O, C) of Jurassic aragonitic shells from England and NW Poland: palaeoecologic and environmental implications. *Geobios* 35, 29–39.
- Marshall, J.D., 1992. Climatic and oceanographic isotopic signals from the carbonate rock record and their preservation. *Geol. Mag.* 129, 143–160.
- Mattioli, E., 1997. Nannoplankton productivity and diagenesis in the rhythmically bedded Toarcian–Aalenian Fiuminata section (Umbria–Marche Apennine, Central Italy). *Palaeogeogr. Palaeoclimatol. Palaeoecol.* 130, 113–133.
- Mattioli, E., Pittet, B., 2002. Contribution of calcareous nannoplankton to carbonate deposition: a new approach applied to the Lower Jurassic of central Italy. *Mar. Micropaleontol.* 45, 175–190.
- Mattioli, E., Pittet, B., 2004. Spatial and temporal distribution of calcareous nannofossils along a proximal–distal transect in the Lower Jurassic of the Umbria–Marche Basin (central Italy). *Palaeogeogr. Palaeoclimatol. Palaeoecol.* 205, 295–316.
- McArthur, J.M., Mutterlose, J., Price, G.D., Rawson, P.F., Ruffell, A., Thirlwall, M.F., 2004. Belemnites of Valanginian, Hauterivian and Barremian age: Sr-isotope stratigraphy, composition (87Sr/86Sr,

- $\delta^{13}\text{C}$, $\delta^{18}\text{O}$, Na, Sr, Mg.), and palaeo-oceanography. *Palaeogeogr. Palaeoclimatol. Palaeoecol.* 202, 253–272.
- Melinte, M., Mutterlose, J., 2001. A Valanginian (Early Cretaceous) “Boreal nannoplankton excursion” in sections from Romania. *Mar. Micropaleontol.* 43, 1–25.
- Olivier, N., Pittet, B., Mattioli, E., 2004. Palaeoenvironmental control on sponge-reefs and contemporaneous deep-shelf marl–limestone deposition (Late Oxfordian, southern Germany). *Palaeogeogr. Palaeoclimatol. Palaeoecol.* 212, 233–263.
- Padden, M., Weissert, H., Funk, H., Schneider, S., Gansner, C., 2002. Late Jurassic lithological evolution and carbon–isotope stratigraphy of the western Tethys. *Eclogae Geol. Helv.* 95, 333–346.
- Pellenard, P., Deconinck, J.-F., Huff, W.D., Thierry, J., Marchand, D., Fortwengler, D., Trouillier, A., 2003. Characterization and correlation of Upper Jurassic (Oxfordian) bentonite deposits in the Paris Basin and the Subalpine Basin, France. *Sedimentology* 50, 1035–1050.
- Philippe, M., Thevenard, F., 1996. Distribution and palaeoecology of the Mesozoic wood genus *Xenoxylon*: palaeoclimatological implication for the Jurassic of Europe. *Rev. Palaeobot. Palynol.* 91, 353–370.
- Pittet, B., Mattioli, E., 2002. The carbonate signal and calcareous nannofossil distribution in an Upper Jurassic section (Balingen–Tieringen, Late Oxfordian, southern Germany). *Palaeogeogr. Palaeoclimatol. Palaeoecol.* 179, 71–96.
- Podlaha, O.G., Mutterlose, J., Veizer, J., 1998. Preservation of $\delta^{18}\text{O}$ and $\delta^{13}\text{C}$ in belemnite rostra from the Jurassic/early Cretaceous successions. *Am. J. Sci.* 298, 324–347.
- Poulton, T.P., Dettmerman, R.L., Hall, R.L., Jones, D.L., Peterson, J.A., Smith, P., Tipper, H.W., Westermann, G.E.G., 1992. Western Canada and United States. In: Westermann, G.E.G. (Ed.), *The Jurassic of Circum Pacific*. Cambridge University Press, Cambridge, UK, pp. 29–92.
- Premoli Silva, I., Erba, E., Tornaghi, M., 1989. Palaeoenvironmental signals and changes in surface fertility in mid Cretaceous C_{org} -rich pelagic facies of the Fucoid Marls (Central Italy). *Geobios* 11, 225–236.
- Price, G.D., 1999. The evidence and implications of polar ice during the Mesozoic. *Earth-Sci. Rev.* 48, 183–210.
- Pucéat, E., Lécuyer, C., Sheppard, S.M.F., Dromart, G., Reboulet, S., Grandjean, P., 2003. Thermal evolution of Cretaceous Tethyan marine waters inferred from oxygen isotopes composition of fish tooth enamels. *Paleoceanography* 18. doi:10.1029/2002PA000823.
- Rosales, I., Quesada, S., Robles, S., 2004. Paleotemperature variations of Early Jurassic seawater recorded in geochemical trends of belemnites from the Basque/Cantabrian basin, northern Spain. *Palaeogeogr. Palaeoclimatol. Palaeoecol.* 203, 253–275.
- Roth, P.H., Bowdler, J.L., 1981. Middle Cretaceous calcareous nannoplankton biogeography and oceanography of the Atlantic Ocean. *SEPM, Spec. Publ.* 32, 517–546.
- Roth, P.H., Krumbach, K.R., 1986. Middle Cretaceous calcareous nannofossil biogeography and preservation in the Atlantic and Indian Oceans: implications for paleoceanography. *Mar. Micropaleontol.* 10, 235–266.
- Schrag, D.P., DePaolo, D.J., Richter, F.M., 1995. Reconstructing past sea surface temperatures: correcting for diagenesis of bulk marine carbonate. *Geochim. Cosmochim. Acta* 59, 2265–2278.
- Seyed-Emani, K., Schairer, G., Zeiss, A., 1995. Ammoniten aus der Dalichai Formation (Mittlere bis Oberer Jura) und der Lar-Formation (Oberer Jura) N Emamzadeh-Hashem (Zentralalborz, Nordiran). *Mitt. Bayer. Staatssamml. Paläontol. Hist. Geol.* 35, 39–52.
- Street, C., Bown, P.R., 2000. Paleobiogeography of Early Cretaceous (Berriasian–Barremian) calcareous nannoplankton. *Mar. Micropaleontol.* 39, 265–291.
- Thierstein, H.R., 1981. Late Cretaceous nannoplankton and the change at the Cretaceous–Tertiary boundary. *SEPM, Spec. Publ.* 32, 355–394.
- Thierstein, H.R., Roth, P.H., 1991. Stable isotopic and carbonate cyclicity in Lower Cretaceous deep-sea sediments: dominance of diagenetic effects. *Mar. Geol.* 97, 1–34.
- Topchishvili, M., Lominadze, T., Tsereteli, L., 1998. Ammonite associations and biostratigraphy of the Middle Jurassic sediments of Georgia. *Cuad. Geol. Iber.* 24, 293–309.
- Tremolada, F., Van de Schootbrugge, B., Erba, E., 2005. The Early Jurassic Schizosphaerellid crisis: implications for calcification rates and phytoplankton evolution across the Toarcian OAE in Cantabria, Spain. *Paleoceanography* 20. doi:10.1029/2004PA001120.
- Tremolada, F., Erba, E., Bralower, T.J., in press. Late Barremian to early Aptian calcareous nannofossil paleoceanography and paleoecology from the Ocean Drilling Program Hole 641C (Galicia Margin). *Cret. Res.*
- Tribouillard, N.P., Gorin, G., Belin, S., Hopfgartner, G., Pichon, R., 1992. Organic-rich biolaminated facies from a Kimmeridgian lagoonal environment in the French Southern Jura mountains—A way of estimating accumulation rate variations. *Palaeogeogr. Palaeoclimatol. Palaeoecol.* 99, 163–177.
- Van de Schootbrugge, B., Bailey, T.R., Rosenthal, Y., Katz, M.E., Wright, J.D., Miller, K.G., Feist-Burkhardt, S., Falkowski, P.G., 2005. Early Jurassic climate change and the radiation of organic-walled phytoplankton in the Tethys Ocean. *Paleobiology* 31, 73–97.
- Walsworth-Bell, E.B. (2001). Jurassic calcareous nannofossils and environmental cycles. Unpub. PhD thesis, 140 pp. University College London, London, UK.
- Watkins, D.K., 1989. Nannoplankton productivity fluctuations and rhythmically bedded pelagic carbonates of the Greenhorn Limestone (Upper Cretaceous). *Palaeogeogr. Palaeoclimatol. Palaeoecol.* 74, 75–86.
- Weissert, H., Erba, E., 2004. Volcanism, CO_2 and paleoclimate: a Late Jurassic–Early Cretaceous carbon and oxygen isotope record. *J. Geol. Soc. (Lond.)* 161, 695–702.
- Weissert, H., Lini, A., 1991. Ice age interlude during the time of Cretaceous greenhouse climate? In: Müller, D.W., McKenzie, J.A., Weissert, H. (Eds.), *Controversies in Modern Geology*. Academic Press, London, UK, pp. 173–191.
- Wierzbowski, H., 2004. Carbon and oxygen isotope composition of Oxfordian–Early Kimmeridgian belemnite rostra: palaeoenvironmental implications for Late Jurassic seas. *Palaeogeogr. Palaeoclimatol. Palaeoecol.* 203, 153–168.
- Williams, J.R., Bralower, T.J., 1995. Nannofossil assemblages, fine fraction stable isotopes, and the paleoceanography of the Valanginian–Barremian (Early Cretaceous) North Sea Basin. *Paleoceanography* 10, 815–864.
- Ziveri, P., Stoll, H., Probert, I., Klaas, C., Geisen, M., Ganssen, G., Young, J.R., 2003. Stable isotope growth effects in coccolith calcite. *Earth Planet. Sci. Lett.* 210, 137–149.